Fast thickness profile measurement of a thin film by using a line scan charge coupled device camera

Cite as: Review of Scientific Instruments **68**, 4525 (1997); https://doi.org/10.1063/1.1148425
Submitted: 11 August 1997 • Accepted: 10 September 1997 • Published Online: 04 June 1998

N. Y. Liang and C. K. Chan

Fast thickness profile measurement of a thin film by using a line scan charge coupled device camera

N. Y. Liang
Department of Physics, National Taiwan University, Taipei, Taiwan, Republic of China

C. K. Chan[a)]
Institute of Physics, Academia Sinica, Nankang, Taipei, Taiwan 11529, Republic of China

(Received 11 August 1997; accepted for publication 10 September 1997)

A technique based on counting the interference fringes produced by a thin film with a fast line scan charge coupled device camera is developed to measure the thickness profiles of the film every 50 μS. When this technique is applied to the bursting of a soap film, the dynamics of the bursting can be reconstructed from these thickness profiles. A method of thickness calibration by using a white light laser as a multiwavelength light source and a video camera as a detector is also introduced. The merit of this calibration technique is that with the help of digital image processing nearly no alignments of the optics are needed. © *1997 American Institute of Physics.*
[S0034-6748(97)03012-8]

I. INTRODUCTION

The measurement of the thickness of a thin film is a common but important task in understanding the properties of thin films. Usually, the techniques of reflectometry[1] and ellipsometry[2] are used to obtain the thickness of a thin film. These two techniques usually provide information of thickness at a point on the film because the commonly used detectors such as photodiodes and photomultipliers are point detectors. Therefore, in order to obtain thickness profiles of the film along some directions, the measuring point must be relocated by either moving the optics or the sample. Since mechanical movements are involved, these techniques are inherently slow and are only applicable for static films or when the changes in the thickness of the film under measurement are slow compared to the measuring time. However, in the situations where fast dynamics occur, a much faster measuring technique is required. For example, during the bursting of a soap film,[3] the thickness profiles of the film changes in a matter of a few milliseconds. In order to obtain the dynamics of the bursting process, thickness profiles must be measured at least every 0.1 ms.

To obtain thickness information of a thin film in such a short time, one can rely on the interference fringes produced by the reflection of light on the thin film if the thickness of the film is of the order of the wavelength of light. Each interference fringe thus formed is the contour of constant thickness. Therefore, if images of the interference fringes can be acquired very rapidly, the thickness information at very short time intervals can be obtained. In order to obtain these pictures, a fast motion mechanical camera or fast video camera can be used. For the fast mechanical cameras, a frame rate as high as 10^5 frames/s[4] can be attained. However, the use of the fast motion camera is very expensive and inconvenient; one cannot adjust experimental settings *in situ* and has to wait for the developing of the negatives. In the case of fast video cameras, no negatives are needed and a frame rate as high as 10^4 frames/s is possible. But the spatial resolution at such a high frame rate is usually very poor (limited to 64×64 pixels^2) because of limited data transfer rate.[5] The above limitations occur when a whole image is needed. However, if only the thickness profiles along one line on the film are needed, an inexpensive line scan charge coupled device (CCD) camera can be used.

In this article, a technique based on measuring the interference fringes produced by a thin film with a fast line scan CCD camera to obtain the thickness profiles of the film at very short interval of time is described. With this apparatus, the thickness profiles of the bursting of soap film can be measured every 50 μS and the dynamics of the bursting can be reconstructed from these thickness profiles. Detailed analysis of the bursting dynamics is then possible. Finally, a calibration of thickness by using a white light laser as a multiwavelength light source and a common video camera as a detector is also introduced. The merit of this calibration technique is that with the help of digital image processing nearly no alignments of the optics are needed.

II. EXPERIMENT

Figure 1 is the schematic diagram for the bursting experiment. A vertical soap film of size 55 mm (height) $\times$40 mm is formed by pulling a frame made of Plexi-Glas vertically out of a soap solution. Three nylon threads ($\sim\mu$m) are tied to the frame to form a rectangular boundary (the fourth side being the liquid-air interface) inside which the film will be formed. The soap solution is made by dissolving surfactants in a mixture of water and glycerin (63% wt water, 37% wt glycerin).[3] Immediately after the soap film has been formed, the film starts to drain and becomes thinner. As the thickness of the film decreases, interference fringes will be visible on the reflected image on an extended light source. These interference fringes will be used to provide the thickness information of the film. Hence all the experiments are carried out when there are clear interference fringes. Since the location of the interference fringes will be changed when there is flow in the film, the whole setup is kept inside a transparent box to protect the film from the air current in the

a)Electronic mail: phckchan@ccvax.sinica.edu.tw

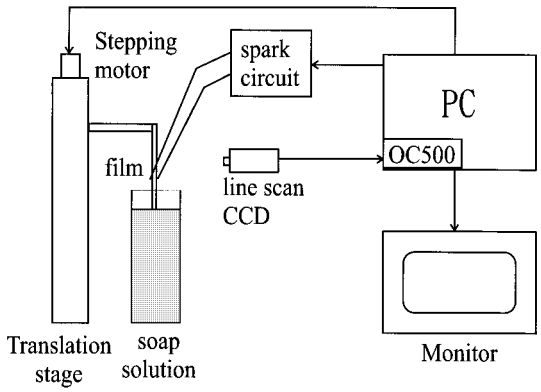

FIG. 1. Schematic diagram for the setup of the experiment.

laboratory. Our goal is to record how these interference fringes are changed during the bursting process of the soap film which will last only for a few milliseconds.

A line scan CCD camera (Dalsa CL-C2-0512)[6] and a frame grabber (OC500)[7] are used to record the position and intensities of the interference fringes along the line $\overline{AB}$ shown in Fig. 2(a). The line is chosen to divide the film into two halves. The line scan CCD camera is different from a common video camera. In a common video camera, there are 525 (for NTSC) scan lines in one video picture. However the line scan camera picture consists of only one single scan line. Therefore, the time interval between two successive pictures in a line scan camera can be much faster than the 1/30 s in the common video camera. In the case of the CL-C2-0512, the line rate can be programmed up to 57 kHz. Because of the fast line rate (short exposure time), the line scan CCD

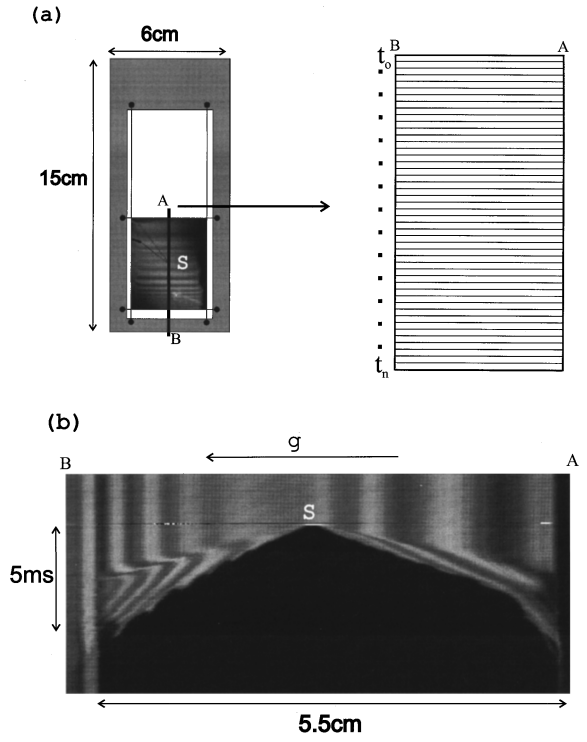

FIG. 2. (a) The scan line on the film and how to form an image from the scan line. (b) A typical image of the bursting process with the scan line shown in (a). *S* is the location of the ignition of a spark.

camera usually has a higher sensitivity than the common video camera. In order to store the pictures obtained from the line scan camera, captured pictures (lines) are combined to form a single frame (two-dimensional image) as shown schematically in Fig. 2(a) where images along the scan line $\overline{AB}$ captured from time t_0 to t_n are combined to form a single frame. This frame contains information of the time evolution of the light intensities along the line $\overline{AB}$ and can be stored in the computer with popular images formats such as TIFF or BMP.

A spark generator, shown in Fig. 1, is used to initiate the bursting process by producing a spark which evaporates the film at a localized point on the film. A typical image of the bursting process as recorded by the line scan CCD camera is shown in Fig. 2(b). Here time is running from top to bottom and gravity is pointing from right to left. The dark and bright strips in the picture are the interference fringes. In the picture, *S* is the point where a spark is ignited to burst the film. The thin horizontal line at *S* is an artifact produced by the electronic interference generated by the spark and provides a good landmark for the origin of the bursting process. Before the spark, it can be seen that the interference fringes are running parallel vertically indicating that there are no changes in thickness before the spark. However, after the spark the scan lines contain an increasing portion of a dark area (hole) which is due to the loss of reflected intensity because of the bursting. Thus, the boundaries between the gray and dark regions in Fig. 2(b) define the trajectory of the bursting rim. Also, there are variations in the positions of the interference fringes which suggests that there are changes in the thickness of the film. Since the interference fringes are the contours of the thickness variations, the profiles of the film along the scanning direction can be determined if the thickness of these fringes are known.

III. CALIBRATION

In order to explain the mapping process between the interference fringes and the film thickness seen in Fig. 2(b), some of the useful results of the interference theory of a thin film[1] will be reviewed. Consider a uniform film of thickness δ and refractive index n located in a medium of refractive index n_1. The reflectivity R of a light ray (with the polarization perpendicular to the incident plane) of wavelength λ, reflected by the film with angle of incidence θ_1 is given by

$$R=\frac{2r^2(1-\cos\,\Delta)}{1+r^4-2r^2\,\cos\,\Delta}. \tag{1}$$

Here the optical path difference Δ is

$$\Delta=\frac{2\pi}{\lambda}2n\delta\,\cos\,\theta \tag{2}$$

and the reflectance r^2 is

$$r^2=\left|\frac{n\,\cos\,\theta-n_1\,\cos\,\theta_1}{n\,\cos\,\theta+n_1\,\cos\,\theta_1}\right|^2. \tag{3}$$

The angle θ is related to θ_1 by $n_1\,\sin\,\theta_1=n\,\sin\,\theta$. The above equations state that only for films with thickness thinner than

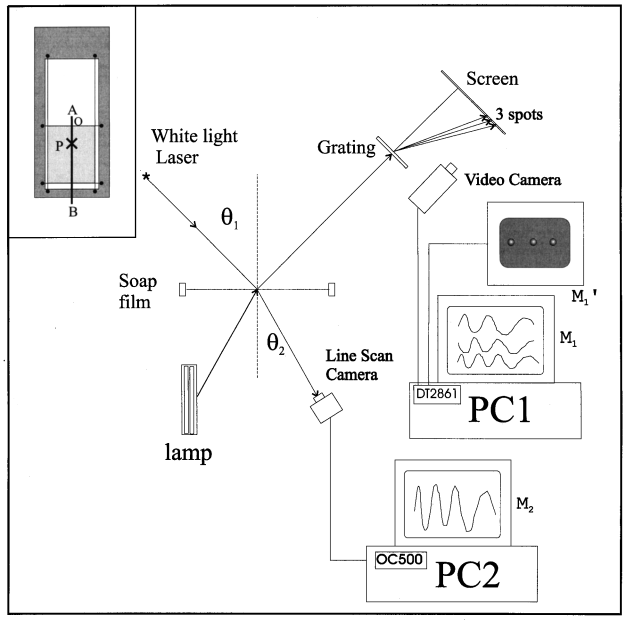

FIG. 3. Schematic diagram showing the calibration process.

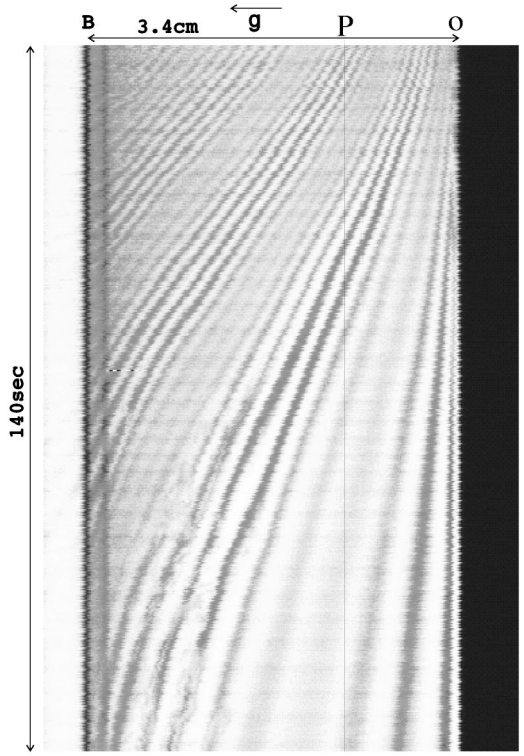

FIG. 4. Typical line scan image for the draining process used in the calibration procedure. Here, P is the point where the white line laser hits the film.

$\lambda/(4n\cos\theta)$ can be determined unambiguously from its reflectivity measurement. For thicker films, the reflectivity is a periodic function of the thickness. Therefore the measurement of reflectivity at a single wavelength cannot determine the thickness uniquely. Traditionally, a lamp which emits light with different wavelengths is used to perform the thickness measurement.[8] The idea is to use the measured reflectivity at different wavelengths to determine the thickness unambiguously. Usually, interference filters of different wavelengths and photodetectors are needed to perform the thickness measurement. This kind of measurement requires the collimation of the light from the lamp and the alignment of the photodetectors with the collimating and detection optics. In our experiments, alignments are needed very often because of the mechanical movement of the film holder and the frequent changes of the film holder. To eliminate the time consuming alignment procedure and the problems mentioned in the below, an image processing technique with a white light laser as a multiple wavelengths light source is developed to calibrate the fringes shown in Fig. 2.

Figure 3 is the schematic diagram for the setup of the thickness calibration of the interference fringes. The idea is to make use of the slow draining process of a soap film to provide slowly varying interference fringes whose thickness can be measured by the method of reflectivity while the images can be recorded by the line scan camera at the same time. The correspondence between the recorded images and the measured thickness is then established to form the calibration. To produce slowly varying fringes, a vertical soap film is pulled out of the soap solution. As mentioned above, thinning takes place immediately after the film has been formed. Two cameras are used to monitor and record this thinning process. The line scan camera scans the soap film in the vertical direction to record the reflected image of a fluorescence lamp along the line $\overline{AB}$. The reason for using a fluorescence lamp is that it has a more or less uniform luminosity across its extended size (10 cm) to produce well-illuminated images of the soap film. Also, because of the spectral properties of the fluorescence lamp, the interference produced will be in groups as explained below. With this scanning configuration, the incident angle θ_2 between the fluorescent lamp and the soap film is 31°. Figure 4 is a typical line scan image of the draining process. The point O, is the top of the soap film and the gravity is from right to left. Time is running again from top to bottom. In Fig. 4, the interference fringes in the top (early time) are closer than the bottom (late time). This shows that the film is thicker at the initial times.

To find out the thickness of the fringes in Fig. 4, the beam of a white light laser is directed to the point P on the vertical soap film with the incident angle $\theta_1 = 44.5°$, and the polarization of the light is perpendicular to the incident plane. The white light laser[9] emits light with three main wavelengths namely, 647, 568, and 488 nm. To measure the reflectivities of the film at the point P with the three wavelengths, a diffraction grating (600 lines/mm) is used to separate the reflected light into different colors and directions. Since the white light laser has a total output power of 25 mW, the separated beams are intense enough to be visible on a screen located behind the grating. Originally, three photodiodes were used to monitor the reflected intensities of these beams. However, it was found that there were strong fluctuations in the output voltages of the diodes because of the motions of the film which resulted in the wandering of the reflected beams. These strong fluctuations can be suppressed by focusing the beams on to the photodiodes. But the results are still far from satisfactory as there were still variations of

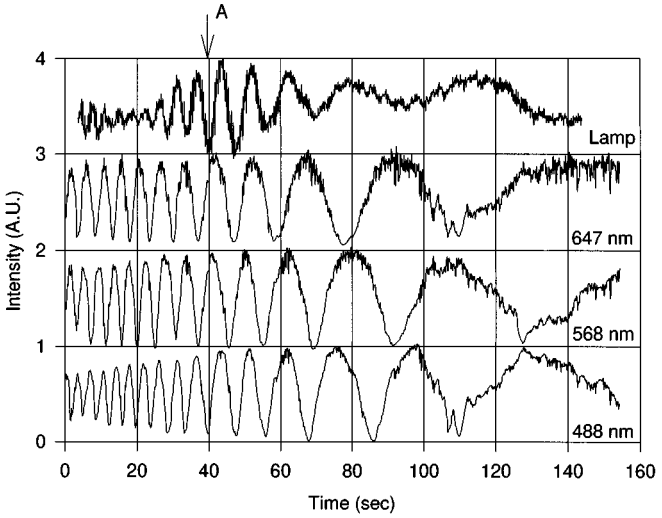

FIG. 5. Time variations of the reflected intensities from the lamp and the three components of the white light laser. All the reflected intensities are normalized to vary between 0 and 1, and the origins of the individual trace are shifted vertically for reason of clarity.

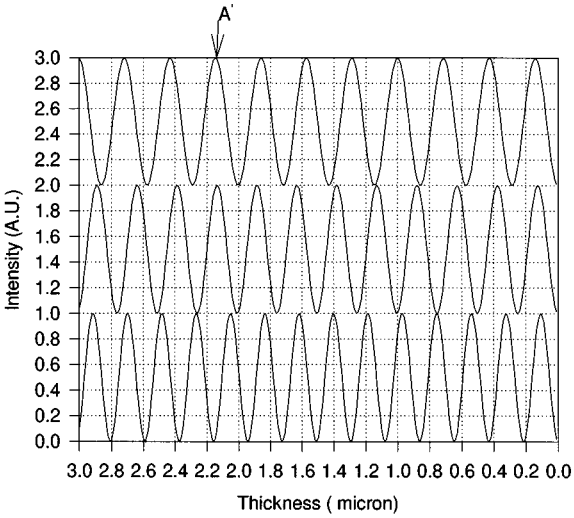

FIG. 6. Theoretical results of the reflected intensities for the three components of the white light laser. All the reflected intensities are normalized to vary between 0 and 1 and the origins of the individual trace are shifted vertically for reason of clarity. Note that the horizontal axis is plotted with thickness decreasing from left to right to facilitate the comparison with Fig. 5.

the diode voltages when there was no obvious changes in the interference fringes.

To solve the beam wandering problem and to eliminate the problem of alignment, a common video camera is used to record the intensities of the three spots appearing on the screen. Images taken by the video camera are fed to the PC1 as shown in Fig. 3. The computer PC1 together with a frame grabber DT2861[10] is used to digitize the image of the three spots and automatically trace the integrated intensities of the three spots inside an area of 20×20 pixels^2 around the three spots such that the reflected spots are always inside their respective areas. With this method, no alignment and focusing are needed and because of the integration, a much more stable signal can be obtained. In Fig. 3, the monitor M_1' displays the three spots which are captured from the screen, and the VGA monitor M_1 displays the light intensities of the three spots in real time. One drawback of using a video camera for reflectivity measure is its linearity calibration. However, as will be seen later, this limitation does not pose a problem. Note that this method is possible because of the strong output of the laser. Otherwise, photodiodes or photomultipliers must be used.

In Fig. 4, P is the point where the white light laser hits the film. The intensity variations along a vertical line at P are therefore the time variations of the reflected intensities of the fluorescence lamp at the point P. Since the reflected intensities of three main components of the white light laser at point P are also recorded by the other video camera at the same time, the time variations of these reflected intensities can be put together for comparison as shown in Fig. 5. In the figure, all the reflected intensities are normalized to vary between 0 and 1 and the origins of the individual trace are shifted vertically for reason of clarity. From top to bottom, the traces are the reflected intensities of the fluorescence lamp, the 647, 568, and 488 nm components of the white light laser, respectively. Since the fluorescence lamp is not a monochromatic light source, the behavior of the top trace is difficult to understand. The idea is to use the three traces at the bottom to fix the thickness of the fringes in the top trace.

In Fig. 5, all the three reflectivities from the white light laser go through oscillations which are caused by the thinning of the film with thickness greater than $\lambda/(4n\cos\theta)$. Theoretically, the oscillations of the three intensities should be of constant amplitude and the relative reflected intensities of the three wavelengths can then be used to determine the film thickness. Therefore, when the thickness of the film at various times is known, the horizontal axis in Fig. 5 can then be translated into a thickness scale and the thickness of the fringes in Fig. 4 which pass through the point P (top trace of Fig. 5) can then be fixed. However, it can be seen from Fig. 5 that the amplitudes of the oscillations of the reflected intensities are not constant and are getting larger as the film is getting thinner (later time). Presumably, this is due to the fact that the flow inside the film dies down only when the film becomes thinner and approaches the ideal situation of the theoretical calculations.

As mentioned above, there are deviations of the measured oscillation amplitudes of the reflected intensities from the ideal situation. The relative intensities cannot be used to calculate the thickness of the film. Instead, to extract the thickness information from Fig. 5, one can make use of the relative phase of the oscillations associated with different wavelengths and compare them with theoretical calculations based on the equations above. Here, it has been assumed that there is a phase associated with the reflected intensity which changes from 0° to 180° when its magnitude changes from minimum to maximum. Figure 6 is the theoretical result of the reflected intensities of the three wavelengths of the white light laser as a function of film thickness based on our experimental parameters. In the figure, oscillations similar to those in Fig. 5 but with constant amplitudes can be seen. In order to find out the thickness of a particular dark fringe (minimum intensity), for example, the point A in the top

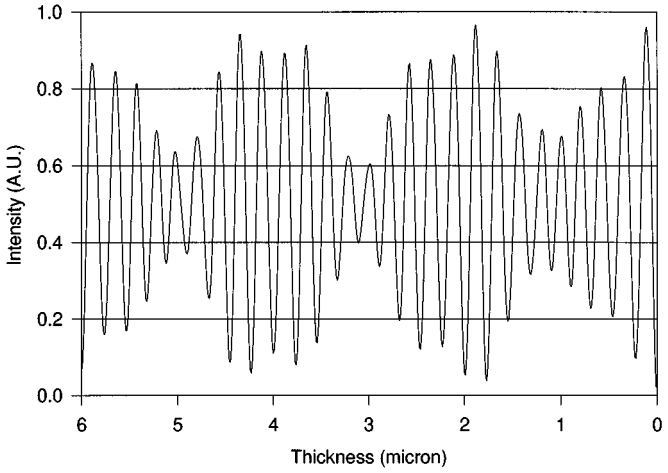

FIG. 7. Simulated interference intensities of the fluorescence lamp as a function of film thickness. Note that the horizontal axis is plotted with thickness decreasing from left to right to facilitate the comparison with Figs. 5 and 6.

trace of Fig. 5, one first notices that the relative phases of the three reflected intensities from the white light laser at the point A are; 180° (max.), 180° (max.), and 0° (min.) from top to bottom, respectively. To map out this thickness, a similar variation of the reflected intensities for these three wavelengths from the theoretical curves in Fig. 6 has to be located. The point A' marked in Fig. 6 is the point which corresponds to the behavior of point A in Fig. 5. Of course, attention must also be paid to the relative position of the neighboring peaks and valleys in Figs. 5 and 6 when such an identification is made. Once the thickness of a single fringe is determined, thickness of all other fringes can be fixed. Therefore, one has just to pick the most unambiguous one to determine its thickness. With this method, the thickness of this particular fringe is determined to be 2.18 μm. When the thickness of each of the fringes in Fig. 4 is known, thickness profiles as a function of time can be constructed.

Another interesting feature of Fig. 4 is that the intensities of the interference fringes seem to be divided into groups. The reason why the reflected intensities from the lamp are separated into groups is that there are about three major lines in the emission of the fluorescence lamp. The grouping is the result of the interference between them. Figure 7 is the simulated result of the variation of the reflected light with different film thickness by using the measured major components of the spectral lines of the light source which are 612, 545, and 436 nm. The intensities in Fig. 7 also get into groups as observed in the experiments above. The grouping is particularly useful when there is a jump in thickness as described below. When the film is thick (3–10 μm), it is easy to determine the thickness of the soap film by simply counting the fringes once the group is known from the white light laser measurement. If a monochromatic light source is used, the grouping will disappear.

In the above analysis, it has been assumed that Fig. 6 can be applied to all the fringes no matter where they are located on the film. However, since pictures are taken from an extended object the angle of incidence will be different for different part of the films and the above method should only

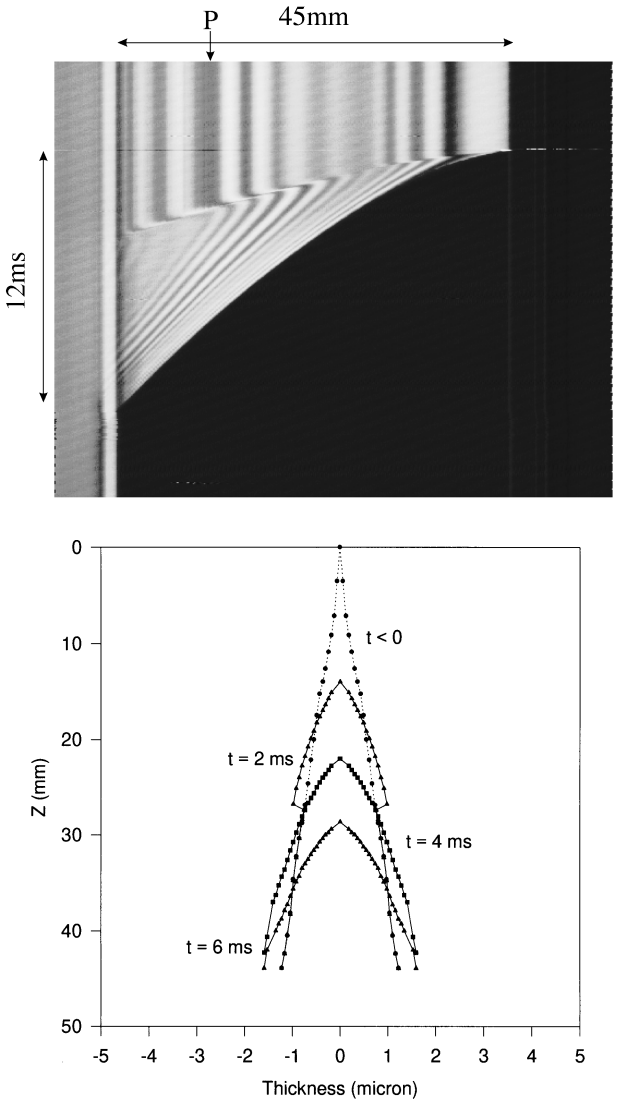

FIG. 8. The bursting of a vertical film of 14 CMC MDW film. (a) The line scan image and (b) the thickness profiles at various times constructed from (a). Here, Z is the vertical direction.

work for the fringes at the center of the film. For example, the angle of incidence of light coming from point B in Fig. 4 is larger than that from point P. A correction must be applied to thickness obtained not in the central part. With the distance between point B and point P being 3 cm and the distance between line scan CCD and soap films being 16 cm, the angle of incidence for light coming from point B is determined to be 32.6°. The angular difference will affect the thickness measurement if not corrected. However, the thickness variation due to this angular difference is found to be below 1% and it will be neglected here.

IV. RESULTS AND DISCUSSIONS

After working with the calibration procedure a couple of times, it is not difficult to tell the approximate thickness of a thinning film by simply looking at the three reflectivity traces from the white light laser displayed on the VGA screen. Therefore, in actual experiments, the white light laser and the video camera are always turned on so that the information

displayed on the VGA screen can be used to determine *in situ* when the desired thickness has been reached and the spark should be ignited. A record of the time variations of these reflectivities similar to Fig. 5 is also saved for each bursting film. This record will be used to calibrate the interference fringes recorded by the line scan CCD camera after the experiment.

To see how this technique is applied to actual experiments, a line scan image of the bursting of a 140 critical micelle concentration (CMC) Moore dish wash (MDW) film[11] is shown in Fig. 8(a). Similar to the line scan images shown above, time is running from top to bottom while gravity is pointing from right to left. Apparently Fig. 8(a) is less noisy when compared to Fig. 4. The noise in Fig. 4 causes uncertainties in the starting time of the scan lines and therefore the edges of the film in Fig. 4 are zigzagged. However, the uncertainties caused by the noises can be removed by translating the scan lines horizontally to some determined position which is known to be straight such as the edges of the frame. Figure 8(a) is the result obtained after the application of this noise removing technique. In Fig. 8(a), the bursting is initiated at the top of the film. The grouping of the interference fringes can be seen. Undisturbed films are marked by parallel vertical stripes. An interesting feature is immediately visible in Fig. 8(a). A front which marks an abrupt change in thickness (twisting of the originally parallel vertical stripes) is running ahead of the bursting rim. The structures in between the undisturbed film and the bursting rim are referred to as the aureole.[3] Figure 8(b) is the thickness profile reconstructed from Fig. 8(a) and shows how the thickness profile changes during bursting. The jump in thickness in front of the bursting front can be clearly seen. Note that the grouping of the fringes is particularly useful in determining the jump in thickness here because the whole group is moved. It is easier to identify the movement of a group of fringes than the movement of just one particular fringe. The abrupt change in thickness in the front of the aureole is produced by the shock wave generated by the bursting process. Evidence of the existence of the shock wave and the aurole was reported some 30 years ago.[3,12] However, it is only with our present technique that the shock wave and the aureole can be so clearly seen and detailed quantitative comparison with the theory can be made. With Fig. 8(a) both the bursting velocity and the shock velocity can be determined. These quantities are of vital importance in the understanding of the bursting of a soap film. Details of the results of the bursting experiments can be found elsewhere.[13]

Finally, it must be noted that our technique is useful only when interference fringes are visible which means that the thickness of the film is of the order of the wavelength of light. Since the calibration procedure does not rely on accurate intensity measurement, the linearity of both the video camera and the line scan camera can be neglected. Even the uniformity of the luminance of the extended light source over the entire film is not required. However, for films with thickness smaller than $\lambda/(4n\cos\theta)$, there will be no interference fringes. In this latter case, the use of the white light laser does not help. One has to rely on the line scan camera to infer the thickness of the film from the measured reflected intensities. In such a case, both the linearity of the line scan camera and the uniformity in luminance of the extended light source must be carefully calibrated. Obviously, in the other extremes, for films with thickness much thicker than the wavelength of light, there will be too many fringes to be distinguishable by the line scan camera.

ACKNOWLEDGMENTS

This work is supported mainly by the National Council of Science of R.O.C. under Grant No. NSC86-2112-M-001-002 and partly by Wong Choi Softech.

[1] See, for example, E. Hecht and A. Zajac, *Optics* (Addison-Wesley, Reading, MA, 1974).
[2] See, for example, R. M. A. Azzam and N. M. Bashara, *Ellipsometry and Polarized Light* (Elsevier, Amsterdam, 1987).
[3] W. R. McEntee and K. J. Mysels, J. Phys. Chem. **73**, 3018 (1969).
[4] For example, the high speed cameras from NAC, 17 Kowa Bldg. No. 2-7, Nishi-Azabu 1-Chome, Minato-ku, Tokyo, Japan.
[5] For example, the high speed motion analyzer, Model 4540 from Kodak, Motion Analysis Systems Division, 11633 Sorrento Valley Rd., San Diego, CA 92121-1097.
[6] Dalsa Inc., 605 McMurray Road, Waterllo, Ontario, N2V 2E9, Canada.
[7] Coreco Inc., 6969 Trans-Canada Hwy, Suite 113, St-Laurent, Quebec, H4T 1V8, Canada.
[8] See, for example, P. Pieranski, L. Beliard, J.-Ph. Tournellec, X. Leoncini, C. Furtlehner, H. Dumoulin, E. Fiou, B. Jouvin, J.-P. Fenerol, Ph. Palaric, J. Heuving, B. Cartier, and I. Kraus, Physica A **194**, 364 (1993).
[9] Model 60, American Laser Corporation, 1832 South 3850 West, Salt Lake City, Utah 84104.
[10] Data Translation, 100 Locke Drive, Marlboro, MA 01752-1192.
[11] For detailed descriptions of the surfactant, please see Ref. 13.
[12] I. Liebman, J. Corry, and H. E. Perlee, Science **161**, 373 (1968).
[13] N. Y. Liang, C. K. Chan, and H. J. Choi, Phys. Rev. E **54**, R3117 (1996).